NUCL SCI TECH (2019) 30:126
https://doi.org/10.1007/s41365-019-0652-9

An efficient method for mapping the $^{12}C + ^{12}C$ molecular resonances at low energies

Xiao-Dong Tang[1,2] · Shao-Bo Ma[1,2] · Xiao Fang[3] · Brian Bucher[4] · Adam Alongi[5] · Craig Cahillane[5] · Wan-Peng Tan[5]

Received: 30 April 2019 / Revised: 17 May 2019 / Accepted: 23 May 2019 / Published online: 13 July 2019

Abstract The $^{12}C+^{12}C$ fusion reaction is famous because of its complication of molecular resonances, and it plays an important role in both nuclear structural research and astrophysics. It is extremely difficult to measure the cross sections of $^{12}C+^{12}C$ fusions at energies of astrophysical relevance because of the very low reaction yields. To measure the complicated resonant structure that exists in this important reaction, an efficient thick target method has been developed and applied for the first time at energies $E_{c.m.} < 5.3$ MeV. A scan of the cross sections over a relatively wide range of energies can be carried out using only a single beam energy. The result of measurement at $E_{c.m.} = 4.1$ MeV is compared with results from previous work. This method will be useful for searching for potentially existing resonances of $^{12}C + ^{12}C$ in the energy range 1 MeV $< E_{c.m.} < 3$ MeV.

Keywords $^{12}C+^{12}C$ · Molecular resonance · Thick target method · $^{12}C(^{12}C, p)^{23}Na$

1 Introduction

The $^{12}C+^{12}C$ fusion reaction is famous because of its complicated molecular resonances and its importance in nuclear astrophysics [1–3]. The mechanism of these strong resonant structures has been studied and discussed by many experimental and theoretical works [1, 2, 4–17]. The $^{12}C+^{12}C$ fusion reaction at low energies plays important roles in nucleosynthesis during the stellar evolution of massive stars and is considered to ignite a carbon–oxygen white dwarf into a type Ia supernova explosion [18, 19]. The effective energy of carbon burning is approximately from 1 to 3 MeV (Gamow window) [18], at which the cross section varies from 10^{-21} to 10^{-7}b. Therefore, it is extremely difficult to directly measure the $^{12}C+^{12}C$ fusion cross sections at stellar energies. Lacking a clear understanding of the complicated resonances in the $^{12}C+^{12}C$ fusion cross section, one cannot reliably extrapolate the cross sections down to the unmeasured stellar energies. Despite more than five decades of studies [1, 2, 4–16], the $^{12}C+^{12}C$ fusion cross sections at stellar energies are still highly uncertain. Measurements that are more precise are urgently needed, especially at stellar energies, to understand the resonance-like structure and provide more reliable cross-sectional data for astrophysical applications.

This work was supported by the National Key R&D Program of China (No. 2016YFA0400500), the National Natural Science Foundation of China (Nos. 11805291, 11475228, 11490560, 11490564, 11875329), the National Science Foundation of the US (Nos. PHY-1068192, PHY-1419765), the US Department of Energy (No. DE-AC07-05ID14517), the Key Program (No. XDPB09-2) and the "Hundred Talents Program" of the Chinese Academy of Sciences, and the Fundamental Research Funds for the Central Universities (No. 18lgpy84).

✉ Xiao Fang
fangx26@mail.sysu.edu.cn

[1] Institute of Modern Physics, Chinese Academy of Sciences, Lanzhou 730000, China

[2] School of Nuclear Science and Technology, University of Chinese Academy of Sciences, Beijing 100049, China

[3] Sino-French Institute of Nuclear Engineering and Technology, Sun Yat-sen University, Zhuhai 519082, China

[4] Idaho National Laboratory, Idaho Falls, ID 83415, USA

[5] Institute for Structure and Nuclear Astrophysics, University of Notre Dame, Notre Dame, IN 46556, USA

Both thin and thick targets have been used in experiments measuring the $^{12}C+^{12}C$ fusion cross sections. Thin carbon foils with thicknesses of a few tens of μg/cm^2 are usually used to measure the resonant structure and cross sections of the $^{12}C+^{12}C$ fusion reaction at relatively high energies. However, this type of target suffers from carbon buildup on its surface, which increases the target thickness continuously during an experiment and brings significant discrepancies into the results. In addition, the small cross sections at stellar energies demand a high-intensity ^{12}C beam ($> 10 p\mu A$). The thin carbon foils are easily damaged by such high-current beams. In the thick target approach, the beam is fully stopped inside the target and the thick target yield is measured. The cross section is then obtained by calculating the derivative (dY/dE) from the measured thick target yield. The typical resonance width in the $^{12}C+^{12}C$ excitation function is approximately 50 keV or less. To precisely map the resonant structures, fine energy steps (e.g., $\Delta <$ 100 keV in the laboratory frame) are required. The yield difference between two adjacent energy points $Y(E)$ and $Y(E-\Delta)$ is calculated to determine the dY/dE. Because the thick target yields only slightly changes within a fine energy step Δ, reasonably high statistics is required for each yield to obtain a reliable derivative for determination of the cross section.

In the present study, a new thick target approach is developed based on an analysis of the $^{12}C(^{12}C, p)^{23}Na$ reaction. A scan of the cross sections over a relatively wide range of energies can be carried out using a single, constant beam energy. By contrast, conventional methods require more than 10 energy points with fine steps to accomplish such a task. This new approach is much more efficient at mapping the $^{12}C+^{12}C$ resonance structure and is extremely useful in searching for new resonances at stellar energies.

The paper is organized as follows: First, we introduce a thick target experiment for $^{12}C+^{12}C$. Second, the principle of the new thick target method is explained and validated with a detailed Monte Carlo simulation by Geant4. Third, we apply this method to analyze the $^{12}C(^{12}C,p_1)^{23}Na$ reaction. Fourth, the experimental results obtained with this thick target method are compared with a measurement using the traditional thin target. Finally, the strengths and weaknesses of the thick target method are discussed.

2 The $^{12}C(^{12}C, p)^{23}Na$ experiment

The $^{12}C(^{12}C, p)^{23}Na$ reactions were measured by experiments in the center of mass energy range of 3–5.3 MeV using thick targets. A ^{12}C beam with an intensity of up to 1 pμA was provided by the 10 MV FN Tandem accelerator at the University of Notre Dame. A gas stripper system was used to enhance the intensity of the 2^+ charge state. The beam energies were determined by measuring the magnetic field of an analyzing magnet after the accelerator. The magnet was calibrated using the $^{27}Al(p,n)$ and $^{12}C(p,p)$ reactions.

The setup for the present experiment is shown in Fig. 1. Two 500-μm-thick YY1-type silicon detectors from Micron Semiconductor Ltd. were placed at backward angles from 113.5° to 163.5° in the laboratory frame. For the $^{12}C+^{12}C$ fusion reaction at energies below the Coulomb barrier, the most important two reaction channels are $^{12}C(^{12}C, p)^{23}Na$ and $^{12}C(^{12}C,\alpha)^{20}Ne$. Each detector was covered with a 12.7-μm-thick Al foil in the front to completely stop the α particles emitted from the $^{12}C(^{12}C,\alpha)^{20}Ne$ reaction. One detector surface was perpendicular to the beam direction covering the angular range 143.5° to 163.5°, and the other detector surface held a 54.4° angle with respect to the beam direction, covering from 113.5° to 143.5°. Each wedge-shaped YY1 detector was segmented into 16 strips on the front side. Thus, the angular resolution for charged particles was approximately 1.8°. The detectors were calibrated using an Am-Cd mixed α source. The energy resolution for an individual strip was approximately 40 keV (FWHM) for 5.486-MeV α particles. The total solid angle of silicon detectors was determined to be 2.59% of 4π. A ^{12}C beam with an intensity of $\sim$0.5–1 pμA was used to bombard a natural graphite target having a thickness of 1 mm.

3 The principle of the thick target method

Consider a reaction,

$$A + a \rightarrow B + b + Q, \quad (1)$$

where Q is the reaction energy, which means the energy produced or absorbed by this reaction. The Q-value for

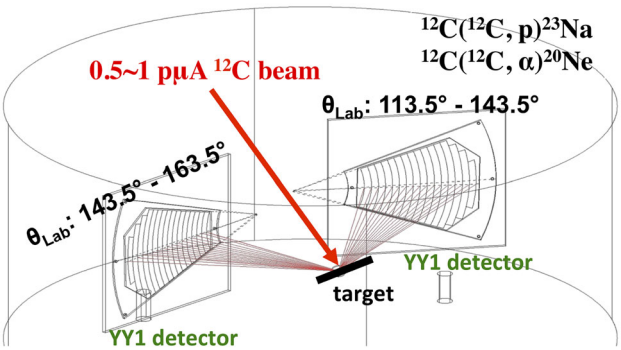

Fig. 1 The setup for the present experiment is shown. Two wedge-shaped silicon strip detectors cover the angles from 113.5° to 163.5° in the laboratory frame

reaction $A(a,b)B$ is the total kinetic energy difference between the initial and final states. It can be determined by

$$Q = \left(\frac{M_a}{M_B} - 1\right)E_a + \left(\frac{M_b}{M_B} + 1\right)E_b - 2\frac{\sqrt{M_a M_b E_a E_b}}{M_B}\cos\theta, \quad (2)$$

where M_a, M_b, and M_B are the masses in amu of the beam, ejectile, and residual particles, respectively; E_a is the beam energy and E_b is the energy of the ejectile particle b; θ is the outgoing angle of b. The values of E_b can be measured by detectors.

The principle of the thick target method for $^{12}C(^{12}C, p)^{23}Na$ is shown in Fig. 2. An infinitely thick target (i.e., thickness much greater than the beam range inside the target material) is used in this method. The ^{12}C beam particles, with incident energy E_{beam}, bombard the target. As they collide with the target nuclei, they continuously lose energy, until they either react with a target nucleus or stop within a distance of a few μms under the front surface of the target. The ranges of the ^{12}C beam in the ^{12}C target are approximately 5.7 and 7.1 μm for E_{beam}= 8 and 10 MeV, respectively. When the $^{12}C(^{12}C, p)^{23}Na$ reaction occurs, the actual energy of the ^{12}C beam is unknown. Protons produced at backward angles can easily penetrate through the target surface with an insignificant energy loss and reach the silicon strip detectors. The energies and outgoing angles of these protons are recorded by detectors. Two examples of protons, m and n, are shown in Fig. 2. Because the range of the ^{12}C beam in the ^{12}C target is quite small, the outgoing angles of protons [e.g., $(180 - \theta_m)$, $(180 - \theta_n)$] were only determined from the strip numbers of detectors. If the Q-value is known for each individual proton group ($Q = 2.24$ MeV for p_0, $Q = 2.24 - 0.44 = 1.80$ MeV for p_1, etc.), from the measured proton energies in the silicon (accounting for energy loss in the Al degrader foil) and outgoing angles $(180 - \theta_m$, or $180 - \theta_n)$, the actual reaction energy (E'_m, E'_n) can be reconstructed by solving Eq. 2. Therefore, a range of reaction energies $[E_{beam} - \Delta E, E_{beam}]$ is scanned with a single, constant beam energy. The effective width of the scan, ΔE, usually spans from 500 to 800 keV, depending on the clear identification of the reaction for events from each channel. This will be discussed later using the measurement result for $^{12}C(^{12}C,p_1)^{23}Na$.

The kinematic calculation of the $^{12}C(^{12}C, p)^{23}Na$ reaction is shown in Fig. 3. The emitted protons are labeled p_i, corresponding to the i_{th} excited state $(i = 0, 1, 2, 3\ldots)$ populated in the heavy residual ^{23}Na nucleus. For example, p_0 corresponds to ^{23}Na in its ground state, and p_1 to the first excited state, etc. Note that p_0 and p_1 possess significantly more energy than any of the other proton groups (e.g., p_2, p_3, p_4, p_5, etc.). The α-channel has similar rules, with emitted α particles and heavy residual ^{20}Ne nuclei.

The target yield derivative dY/dE is computed for each reaction energy bin after normalizing the count by the total number of incident ^{12}C particles. The cross section for the $^{12}C(^{12}C,p_i)^{23}Na$ reaction is then calculated from the extracted dY/dE using the following equation

$$\sigma(E) = \frac{1}{\varepsilon f N_A}\frac{M_T}{}\frac{dY}{dE}\frac{dE}{d(\rho X)}, \quad (3)$$

where ε is the detection efficiency, which is the geometric efficiency determined by an α source; M_T is the molecular weight of the target nucleus; f is the molecular fraction of the target nucleus; N_A is Avogadro's number; and $dE/d(\rho X)$ is the stopping power, calculated with the SRIM code [20].

For ease of comparison with other experimental data sets, the measured cross sections from this experiment are

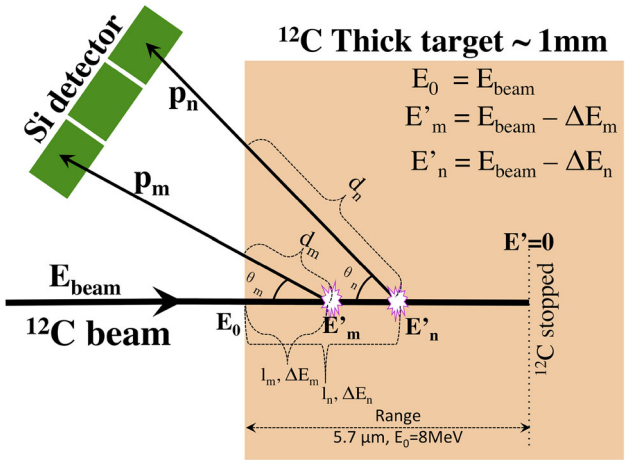

Fig. 2 The principle of the thick target method for the $^{12}C(^{12}C, p)^{23}Na$ reaction. For clarity, the dimensions in this figure are not drawn to scale

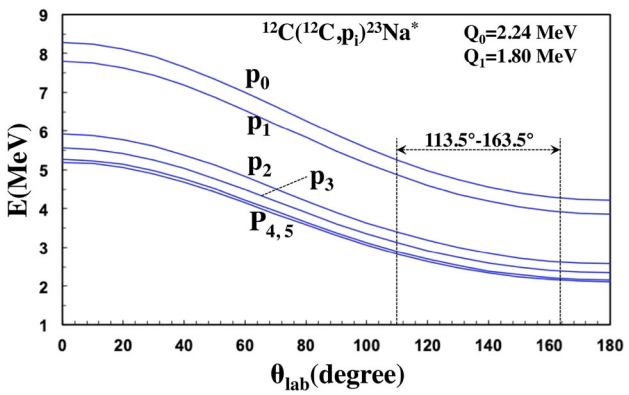

Fig. 3 The kinematic calculation of the $^{12}C(^{12}C, p)^{23}Na$ reaction at $E_{lab} = 8.2$ MeV. The energies of protons at different outgoing angles are given. The protons (p_i) associated with ^{23}Na in its ground and lowest excited states are identified

converted into S^* factors [7], which are defined by the following equation

$$S^* = \sigma E_{\text{c.m.}} \exp\left(\frac{87.21}{\sqrt{E_{\text{c.m.}}}} + 0.46 E_{\text{c.m.}}\right), \quad (4)$$

where σ is the cross section and $E_{\text{c.m.}}$ is the energy in the center of mass frame.

To validate the proposed thick target method, a Geant4 simulation was performed to generate a reaction energy spectrum from a constant S^* factor input ($S^* = 2 \times 10^{16}$ MeV*b). In the simulation, all details introduced above were considered, including the geometry of the detectors, the aluminum degrader, and beam straggling. The reaction energy spectrum from the simulation of the p_1 group with an incident energy of 8.2 MeV is shown in Fig. 4.

4 Obtaining the S^* factor of $^{12}C(^{12}C, p_1)^{23}Na$ with the thick target method

The measurement utilizing the thick target method was carried out in the energy range 3 MeV $< E_{\text{c.m.}} <$ 5.3 MeV (6 MeV $< E_{\text{beam}} <$ 10.6 MeV). The measured results at $E_{\text{beam}} = 8.2$ MeV are shown in Fig. 5.

The reaction Q-value spectrum is computed from Eq. 2 with a constant incident energy of $E_a = 8.2$ MeV. Because

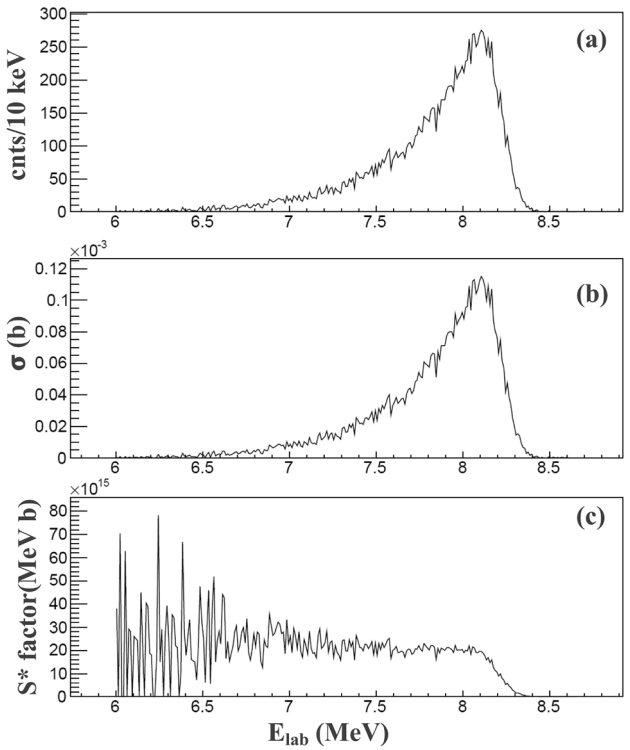

Fig. 4 The simulation results of a 8.2-MeV ^{12}C beam bombarding a thick target. **a** Reconstructed reaction energy spectrum; **b** derived cross sections; **c** derived S^* factors

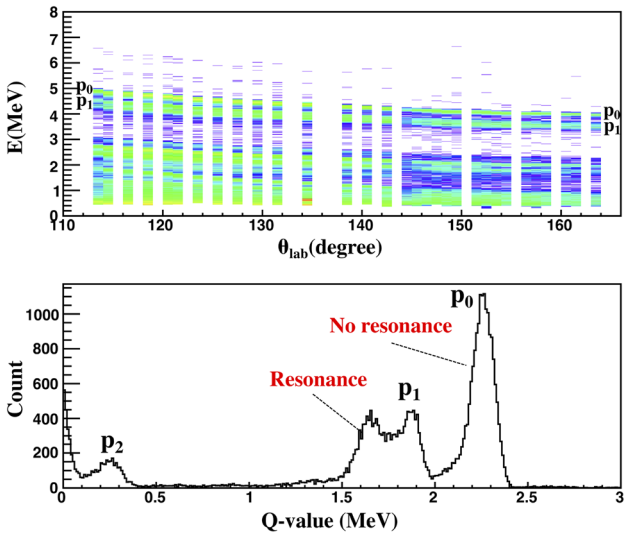

Fig. 5 The experimental spectra measured at $E_{\text{beam}} = 8.2$ MeV using the thick target method. (Top) Energy versus angle of detected protons; (Bottom) the Q-value for the $^{12}C(^{12}C,p_{0,1,2})^{23}Na$ reaction. The events between 2 and 2.4 MeV are from the p_0 channel. The events between 1 and 2 MeV mostly correspond to the p_1 channel, with minor contamination from the p_0 channel

the ^{12}C beam loses its energy as it passes through the target medium, the actual beam energy varies from the initial incident beam energy (8.2 MeV) down to 0. As a result, the shape of the Q-value spectrum becomes much wider and more complicated than the simple sharp Gaussian shape obtained from measurement with a thin target.

The corresponding Q-values of the $^{12}C(^{12}C,p_{0,1,2})^{23}Na$ channels are 2.24, 1.80, and 0.164 MeV, respectively. The large Q-value difference between the p_1 and p_2 channels offers an excellent clear region for identification of the p_1 events. In the present work, we focused on analysis of the p_1 channel. The Q-value spectrum obtained with a thin target is expected to be narrowly 1.80 MeV. However, in the thick target method, as the reaction energy decreases in the target, the energies of the p_1 channel events at each fixed angle extend toward lower values, as shown in the energy versus angle plot (Fig. 5). The p_1 channel events obtained with the thick target form a wide Q-value spectrum when we compute the Q-value using a fixed beam energy, $E_a = 8.2$ MeV.

The Q-value of the p_0 channel also has a low-energy tail, similar to the p_1 channel. These low-energy events from the p_0 channel interfere with the high-energy events from the p_1 channel. As shown in Fig. 5, this is not a huge problem at $E_{\text{c.m.}} = 4.1$ MeV because the p_0 cross section quickly decays with decreasing beam energy. However, the tail of the p_0 channel events may contribute to the events of the p_1 channel around 20% at $E_{\text{c.m.}} = 10.6$ MeV.

By following the procedure introduced above, the reaction energy can be computed for each event using the

p_1 Q-value = 1.80 MeV. The reaction energy spectrum is shown in Fig. 6. Using this unique Q-value for p_1, only reaction energies of events from the p_1 channel are correctly constructed. These events are distributed in the range of the actual reaction energies from 7.0 to 8.2 MeV. Meanwhile, all the events from other channels are placed at the 'wrong' energies. If we wanted to investigate the p_0 channel, Q-value = 2.24 MeV should be used instead of 1.80 MeV to properly reconstruct the reaction energy.

The energy calibration is crucial for determination of the actual reaction energy in this approach. Considering the uncertainties in the detector energy calibration and the degrader thickness, a minor tuning of the energy shift was applied to the reconstructed reaction energy obtained from the experiment to match the S^* factors at the edge of the high-energy sides between the experimental and simulated spectra.

The present S^* factor measurement using the thick target method is shown in Fig. 7. For the p_1 channel, the maximum reaction energy is $E_{\text{c.m.}} = 4.0$ MeV. The smearing of the edge at 4.1 MeV is a result of the limited resolution of the detectors and the spread of the beam energy. The effective measurement of the S^* factor for the p_1 channel stops at approximately $E_{\text{c.m.}} = 3.4$ MeV, where the background events begin to take over. These background events lead to a quickly rising S^* factor below $E_{\text{c.m.}} = 3.4$ MeV.

5 Comparison with the conventional thin target measurement

The present S^* factor for the p_1 channel at energies from 3.4 to 4.0 MeV is shown in Fig. 8, compared with an earlier measurement using the conventional thin target method by Becker et al. [11]. The highest reaction energy obtained by the thick target method is $E_{\text{c.m.}} = 4.0$ MeV instead of $E_{\text{c.m.}} = 4.1$ MeV because of the smearing effect resulting from the limited energy and angular resolution. It is impressive that the complicated resonant structure of the p_1 channel through a wide energy range can be easily revealed with a single incident beam energy using the thick target method. A scan of approximately ten energy points is required if using the conventional thin target method (or with the differential thick target method). It is also clear that the S^* factor obtained with the thick target method is approximately 50% higher than Becker's data at $E_{\text{c.m.}} = 3.78$ MeV. This is possibly an effect of the angular distribution. In the thick target experiment, we assumed a simple isotropic angular distribution because of the limited detector angular coverage. In the conventional thin target measurement of Becker et al. [11], a set of silicon detectors was used to provide a well-determined angular distribution.

6 Discussion

The thick target method established in the present work requires a clear identification of the reaction channel of each candidate event. For the $^{12}C(^{12}C,p_i)^{23}Na$, both p_0 and p_1 are good candidates because of their high proton kinetic energies and large separation from the lower Q-value channels. The other proton channels, $p_{2,3,4,5,\ldots}$, are too close to each other. It is thus rather difficult to achieve clear identifications of each channel using only their Q-values. Therefore, the particle-gamma coincidence technique is required for identification of the Q-value [21].

The $^{12}C(^{12}C,\alpha)^{20}Ne$ reaction also could be studied by the present thick target method. The $dE - E$ telescope technique is required to identify the α particles from the protons and the ambient background of δ-electrons. The separation between α_0 and α_1, or between α_1 and α_2, is more significant than that in the p channels. This would provide a better identification of the reaction channel of each α event. However, the energies of these α particles are below 5 MeV at backward angles, and the energy loss of α particles is significant inside the carbon target and Al degrader; the latter is often used in front of the detector to shield scattered ^{12}C particles. A more careful correction is

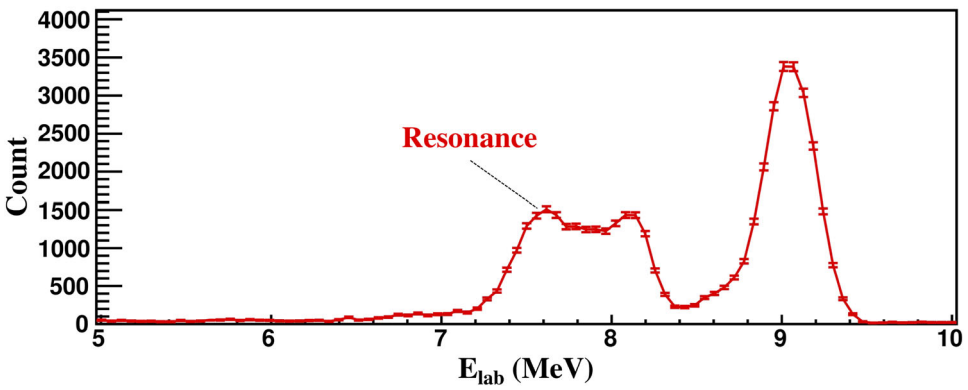

Fig. 6 The reaction energy spectrum constructed from the p_1 Q-value= 1.80 MeV. The true p_1 events are distributed in the range from 7 to 8.2 MeV. All events corresponding to other channels appear with incorrect energy values

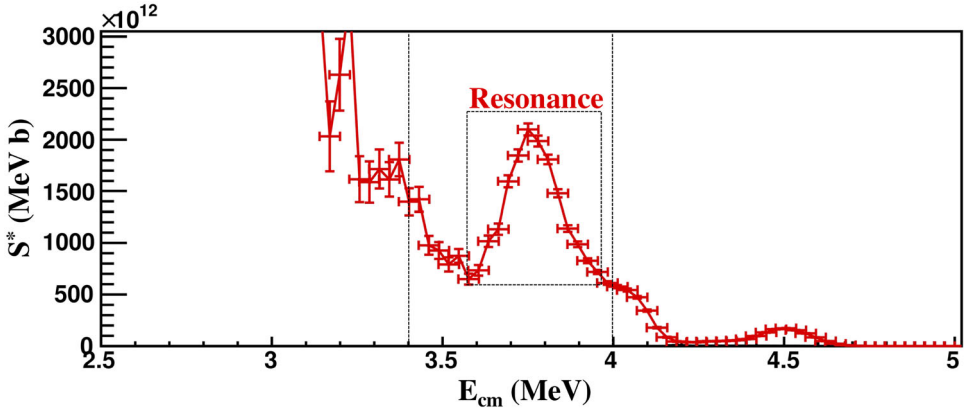

Fig. 7 The S^* factor of the p_1 channel. The effective range of $E_{c.m.}$ is from 3.4 to 4.0 MeV

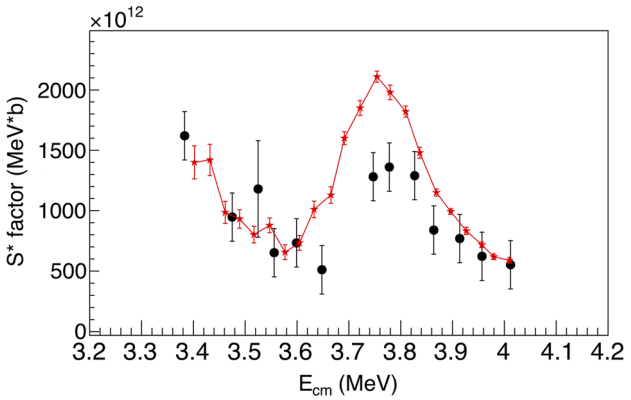

Fig. 8 The S^* factor of the p_1 channel of $^{12}C(^{12}C, p)^{23}Na$. Present results are displayed in red, while the data from Ref. [11] are displayed in black. (Color figure online)

needed for the detected energies and angles of the α particles, bringing more uncertainties into the result. The associated straggling is another limitation for the α particle. New techniques, such as a solenoid spectrometer [15], are helpful for α-detection.

A clean background is essential for clear identification of the reaction channel for each event. The graphite target contains the impurity D_2O, which produces a proton background. A clean carbon target, e.g., highly ordered pyrolytic graphite (HOPG) [22], would greatly reduce contributions from target contaminants to background [16, 23, 24]. Direct measurements in nuclear astrophysics benefit from an underground environment, which greatly reduces cosmic ray-induced background noise. The Jinping Underground laboratory for Nuclear Astrophysics (JUNA) [25] in China, which is being constructed and expected to deliver a beam in a few years, would be a suitable place to perform the $^{12}C+^{12}C$ measurement with the ultra-low background of the China Jinping Underground Laboratory (CJPL) [26].

The present thick target method provides an efficient way to map the resonant structure of the $^{12}C+^{12}C$ fusion reactions. An intense beam can be used with such a target to search for rare events at stellar energies. A snapshot of some particular channels can be obtained efficiently with a single constant incident energy. The snapshot provides important guidance for the following detailed energy scan using the thin target method or the differential thick target method, which may reveal more details of the resonances in other reaction channels.

7 Summary

In summary, an efficient thick target method has been applied for the first time to measure the complicated resonant structure existing in $^{12}C(^{12}C, p)^{23}Na$. It can provide cross sections within a range of $[E_{beam} - \Delta E, E_{beam}]$ using a single incident energy E_{beam}. The $^{12}C+^{12}C$ fusion reaction is one of the most important reactions in nuclear astrophysics. The efficient thick target method outlined in the present work will be useful in searching for potentially existing resonances of $^{12}C + ^{12}C$ in the energy range $1\,\text{MeV} < E_{c.m.} < 3$ MeV, where the cross sections are extremely low.

References

1. D.A. Bromley, J.A. Kuehner, E. Almqvist, Resonant elastic scattering of C^{12} by carbon. Phys. Rev. Lett. **4**, 365 (1960). https://doi.org/10.1103/PhysRevLett.4.365
2. E. Almqvist, D.A. Bromley, J.A. Kuehner, Resonances in C^{12} on carbon reactions. Phys. Rev. Lett. **4**, 515 (1960). https://doi.org/10.1103/PhysRevLett.4.515
3. Nuclear Science Advisory Committee, The 2015 long range plan for nuclear science, 2015
4. E.R. Cosman, T.M. Cormier, K. Van Bibber et al., Evidence for a $^{12}C+^{12}C$ collective band in ^{24}Mg. Phys. Rev. Lett. **35**, 265 (1975). https://doi.org/10.1103/PhysRevLett.35.265
5. N. Cindro, F. Coçu, J. Uzureau et al., Evidence for a rotational band in ^{24}Mg and its fragmentation: A rotation-vibration

coupling? Phys. Rev. Lett. **39**, 1135 (1977). https://doi.org/10.1103/PhysRevLett.39.1135
6. H. Chandra, U. Mosel, Molecular configurations in heavy-ion collisions. Nucl. Phys. A **298**, 151–168 (1978). https://doi.org/10.1016/0375-9474(78)90013-1
7. J.A. Patterson, H. Winkler, C.S. Zaidins, Experimental investigation of the stellar nuclear reaction $^{12}C + {}^{12}C$ at low energies. Astrophys. J. **157**, 367 (1969). https://doi.org/10.1086/150073
8. M.G. Mazarakis, W.E. Stephens, Experimental measurements of the $^{12}C+{}^{12}C$ nuclear reactions at low energies. Phys. Rev. C **7**, 1280 (1973). https://doi.org/10.1103/PhysRevC.7.1280
9. M.D. High, B. Čujec, The $^{12}C+{}^{12}C$ sub-Coulomb fusion cross section. Nucl. Phys. A **282**, 181–188 (1977). https://doi.org/10.1016/0375-9474(77)90179-8
10. K.U. Kettner, H. Lorenz-Wirzba, C. Rolfs et al., Study of the fusion reaction $^{12}C+{}^{12}C$ below the Coulomb barrier. Phys. Rev. Lett. **38**, 337 (1977). https://doi.org/10.1103/PhysRevLett.38.337
11. H.W. Becker, K.U. Kettner, C. Rolfs et al., The $^{12}C+{}^{12}C$ reaction at sub-Coulomb energies (II). Z. Physik A **303**, 305–312 (1981). https://doi.org/10.1007/BF01421528
12. L.R. Gasques, L.C. Chamon, D. Pereira et al., Global and consistent analysis of the heavy-ion elastic scattering and fusion processes. Phys. Rev. C **69**, 034603 (2004). https://doi.org/10.1103/PhysRevC.69.034603
13. E.F. Aguilera, P. Rosales, E. Martinez-Quiroz et al., New γ-ray measurements for $^{12}C+{}^{12}C$ sub-Coulomb fusion: toward data unification. Phys. Rev. C **73**, 064601 (2006). https://doi.org/10.1103/PhysRevC.73.064601
14. T. Spillane, F. Raiola, C. Rolfs et al., $^{12}C+{}^{12}C$ fusion reactions near the Gamow energy. Phys. Rev. Lett. **98**, 122501 (2007). https://doi.org/10.1103/PhysRevLett.98.122501
15. X. Fang, B. Bucher, A. Howard et al., Nucl. Instrum. Methods Phys. Res. A **871**, 35–41 (2017). https://doi.org/10.1016/j.nima.2017.07.050
16. J. Zickefoose, A. Di Leva, F. Strieder et al., Measurement of the $^{12}C(^{12}C, p)^{23}Na$ cross section near the Gamow energy. Phys. Rev. C **97**, 065806 (2018). https://doi.org/10.1103/PhysRevC.97.065806
17. H. Pais, F. Gulminelli, C. Providência et al., Light and heavy clusters in warm stellar matter. Nucl. Sci. Tech. **29**, 181 (2018). https://doi.org/10.1007/s41365-018-0518-6
18. C. Rolfs, W.S. Rodney, *Cauldrons in the Cosmos* (University of Chicago Press, Chicago, 1988)
19. William A. Fowler, Experimental and theoretical nuclear astrophysics: the quest for the origin of the elements. Rev. Mod. Phys. **56**, 149 (1984). https://doi.org/10.1103/RevModPhys.56.149
20. J.F. Ziegler, Website. www.srim.org. Accessed March 2019
21. M. Heine et al., The STELLA apparatus for particle-gamma coincidence fusion measurements with nanasecond timing. Nucl. Instrum. Methods Phys. Res. A **903**, 1–7 (2018). https://doi.org/10.1016/j.nima.2018.06.058
22. C. Soldano, A. Mahmood, E. Dujardin, Production, properties and potential of graphene. Carbon **48**, 2127 (2010). https://doi.org/10.1016/j.carbon.2010.01.058
23. B. Bucher, X. Tang, X. Fang et al., First direct measurement of $^{12}C(^{12}C,n)^{23}Mg$ at stellar energies. Phys. Rev. Lett. **114**, 251102 (2015). https://doi.org/10.1103/PhysRevLett.114.251102
24. X. Fang, W.P. Tan, M. Beard, R.J. deBoer et al., Experimental measurement of $^{12}C+{}^{16}O$ fusion at stellar energies. Phys. Rev. C **96**, 045804 (2017). https://doi.org/10.1103/PhysRevC.96.045804
25. W.P. Liu et al., (JUNA Collaboration), Progress of Jinping Underground laboratory for Nuclear Astrophysics. Sci. China Phys. Mech. Astron. **59**, 642001 (2016). https://doi.org/10.1007/s11433-016-5785-9
26. J.P. Cheng et al., The China Jinping underground laboratory and its early science. Annu. Rev. Nucl. Part. Sci. **67**, 231–251 (2017). https://doi.org/10.1146/annurev-nucl-102115-044842